nonzero C_1 and C_2. We have checked the validity of the assigned errors by making Monte Carlo simulations of a number of statistical samples of 400 and 1000 events. In both cases, the angular distribution used in the Monte Carlo simulation was that of Ref. 12 for 704-MeV incident π^- kinetic energy. It was found that the values of the coefficients resulting from fits to distributions were normally distributed with half-widths equal to the calculated errors. The chance that in a population of 400 parents the given distribution would be mistakenly called isotropic was 1 in 23; for the 1000-event population the chance was 1 in 2000. Thus we conclude that our errors as presented in this paper correctly represent the experimental situation.

PHYSICAL REVIEW VOLUME 187, NUMBER 5 25 NOVEMBER 1969

Spin Analysis of $p\pi^+\pi^-$ Enhancements in the $pp\pi^+\pi^-$ Final State Produced in pp Interactions at 22 GeV/c*

J. I. RHODE, R. A. LEACOCK, W. J. KERNAN, R. A. JESPERSEN, AND T. L. SCHALK
Institute for Atomic Research and Department of Physics, Iowa State University, Ames, Iowa 50010
(Received 28 July 1969)

We have investigated decay angular distributions and other characteristics associated with enhancements near 1450 and 1700 MeV in the $p\pi^+\pi^-$ mass distribution for the $pp\pi^+\pi^-$ final state produced in pp interactions at 22 GeV/c. Our results are consistent with a spin assignment of $\frac{1}{2}$ for the 1450-MeV effect if the $\Delta^{++}\pi^-$ branching of this effect is assumed to be small. We associate this effect with the $P_{11}(1470)$ state inferred from phase-shift analyses. In the case of the 1700-MeV feature, we favor strong contributions from a $J=\frac{5}{2}^+$ state which can be reasonably associated with the $F_{15}(1690)$ state reported in the phase-shift work.

I. INTRODUCTION

IN an analysis of two- and four-prong events from a 75 000-frame exposure of the Brookhaven National Laboratory 80-in. hydrogen bubble chamber to 22-GeV/c protons, we have investigated the following reactions:

$$pp \to pn\pi^+, \quad 220 \text{ events} \quad (1)$$

$$\to pp\pi^+\pi^-, \quad 1234 \text{ events}. \quad (2)$$

Preliminary studies of certain aspects of these final states have been reported previously.[1,2]

We consider here characteristics of two significant enhancements in the $p\pi^+\pi^-$ (and $\Delta^{++}\pi^-$) mass distributions [Fig. 1(a)] for reaction (2), one with mass 1443±15 MeV, width 100±15 MeV, and the second of mass 1693±15 MeV, width 235±50 MeV.[3] We refer to these features as the 1450- and 1700-MeV effects, respectively. Evidence for a two-peak structure in the $p\pi^+\pi^-$ mass spectrum for this and other reactions at various momenta have been noted by other workers.[4–6]

Reaction (2) is characterized by a very strong forward and backward peaking of the final-state baryons in the

* Work performed in part in the Ames Laboratory of the U. S. Atomic Energy Commission. Contribution No. 2598.

[1] R. A. Jespersen, Y. W. Kang, W. J. Kernan, R. A. Leacock, J. I. Rhode, T. L. Schalk, and L. S. Schroeder, Phys. Rev. Letters **21**, 1368 (1968).

[2] R. A. Jespersen, Y. W. Kang, W. J. Kernan, R. A. Leacock, J. I. Rhode, T. L. Schalk, and L. S. Schroeder, in Third Topical Conference on Resonant Particles, Ohio University, Athens, Ohio, 1967 (unpublished).

[3] In quoting masses and widths for these effects we are simply parametrizing features of our data. We can not demonstrate from the $p\pi^+\pi^-$ mass spectrum alone that either of these effects (but especially the 1700-MeV peak) can be associated with a single resonance. In Ref. 1 it was shown that the $p\pi^+\pi^-$ mass distribution for reaction (1) is poorly represented by either a conventional "Deck" background (with or without reasonable refinements in form factors) or by this background plus a single broad resonance. The data are, however, adequately accounted for by two resonance structures plus the Deck background. E. L. Berger *et al.* [Phys. Rev. Letters **20**, 964 (1968)] have shown that a Reggeized Deck calculation is in better agreement with certain features of reaction (1) (at lower momenta) than the original Deck model. Such modifications of the Deck effect are, however, generally unable to account for the sharpness of the 1450-MeV effect seen in our and in certain other workers' data (especially at high energies), and, in any case, cannot reproduce a double-peak structure (see Ref. 6). Nevertheless, these calculations may still be valid, according to the duality concept [R. Dolen, D. Horn, and C. Schmid, Phys. Rev. **166**, 1768 (1968); G. F. Chew and A. Pignotti, Phys. Rev. Letters **20**, 1078 (1968)], in the sense of giving correctly a local average over direct-channel resonance effects. In this view, resonance states in our $\Delta^{++}\pi^-$ channel are already accounted for by (and are not superposed upon) the π trajectory exchange in the crossed channel. If this is correct, then fits to the $p\pi^+\pi^-$ and $\Delta^{++}\pi^-$ mass distributions using resonances plus Deck background will lead to an underestimate of the resonance contribution. Our analysis here is not dependent upon the validity of this approach, although certain arguments in the text, particularly that concerning the $\Delta^{++}\pi^-$ branching of the 1700-MeV effect, are strengthened if this viewpoint is adopted.

[4] S. P. Almeida, J. G. Rushbrooke, J. H. Scharenguivel, M. Behrens, V. Blobel, I. Borecka, H. C. Dehne, J. Diaz, G. Knies, A. Schmitt, K. Strömer, and W. P. Swanson, Phys. Rev. **174**, 1638 (1968).

[5] R. Ehrlich, R. Nieporent, R. J. Plano, J. B. Whittaker, C. Baltay, J. Feinman, P. Franzini, R. Newman, and N. Yeh, Phys. Rev. Letters **21**, 1839 (1968).

[6] J. G. Rushbrooke, in *Proceedings of the Fourteenth International Conference on High-Energy Physics, Vienna, 1968*, edited by J. Prentki and J. Steinberger (CERN, Geneva, 1968), p. 159.

c.m. system.[7] The pions are also forward and backward peaked in the c.m. system, but much less sharply than the baryons. The $p\pi^+\pi^-$ enhancements considered in this report are associated with a reaction process involving production of the $p\pi^+\pi^-$ system moving strongly forward (or backward) in the c.m. frame and having generally low effective mass ($\leq\sim 3000$ MeV). Correspondingly, this $p\pi^+\pi^-$ system is produced at relatively low t with respect to the associated initial-state proton.[8]

We examine the following decay angular distributions for these effects, referred to here loosely as N^*: (1) normal to the N^* decay plane referred to the associated[7] incident-proton direction and determined in the N^* rest frame; (2) direction of the $p\pi^+$ system (mass in Δ^{++} band, 1225 ± 125 MeV) referred to associated-incident-proton direction, again determined in the N^* rest frame; and (3) the π^+ direction (for Δ^{++} decay) referred to the Δ^{++} direction and determined in the Δ^{++} rest system.

An interpretation of the distribution in the normal to the N^* decay plane can be made without consideration of the $\Delta^{++}\pi^-$ decay branching.[9] The sequential decay analysis ($N^*\rightarrow\Delta^{++}\pi^-$, $\Delta\rightarrow p\pi^+$) is more powerful,[9] but is usefully applied only when a significant fraction of the N^* decays go by $\Delta^{++}\pi^-$. To determine the $\Delta^{++}\pi^-$ decay branching we have examined the $p\pi^+$ and $p\pi^-$ mass distributions for events with $p\pi^+\pi^-$ mass in the 1450 ± 50- and 1700 ± 100-MeV regions. The low $p\pi^+\pi^-$ mass of the 1450-MeV cut kinematically constrains the $N\pi$ mass to be in the $\Delta(1238)$ region. In this case both the $p\pi^+$ and $p\pi^-$ mass are peaked nearly symmetrically about the Δ mass [see Fig. 1(d)]. For the 1700 ± 100-MeV $p\pi^+\pi^-$ mass region, however, the $N\pi$ masses are not so constrained; here the $p\pi^-$ mass is peaked much higher. We conclude that though our data are not, in this respect, inconsistent with strong $\Delta^{++}\pi^-$ decay for the 1450-MeV $p\pi^+\pi^-$ region they do, in fact, clearly require it for the 1700-MeV region. Results of fitting both the gross $p\pi^+\pi^-$ mass spectrum and a slightly restricted $\Delta^{++}\pi^-$ distribution[1,3] using resonance terms for effects at 1450 and 1700 MeV plus a Deck background indicate that in our data the contribution of the 1700-MeV feature *above background* is not appreciably reduced by the Δ^{++} selection. This indicates that the 1700-MeV effect, above this background, has a dominant $\Delta^{++}\pi^-$ decay.

Donnachie, in a recent review of results of phase-shift analysis,[10] lists seventeen states below 2000 MeV [excluding $P_{33}(1236)$]. Of these only two states with spin exceeding $\frac{5}{2}$ are listed [an $F_{37}(1950)$ and an $F_{17}(1980)$] of which one is in considerable doubt. All others have spin $\frac{1}{2}$, $\frac{3}{2}$, or $\frac{5}{2}$. Since only $I=\frac{1}{2}$ or $\frac{3}{2}$ N^* states can be produced in the $pp\rightarrow N^*p$ reaction, we expect no contributions in our data from states which are isotopic spin forbidden in the π nucleon channel. We assume, then, that states contributing in the mass region of interest in this report have spin $\frac{1}{2}$, $\frac{3}{2}$, or $\frac{5}{2}$. In

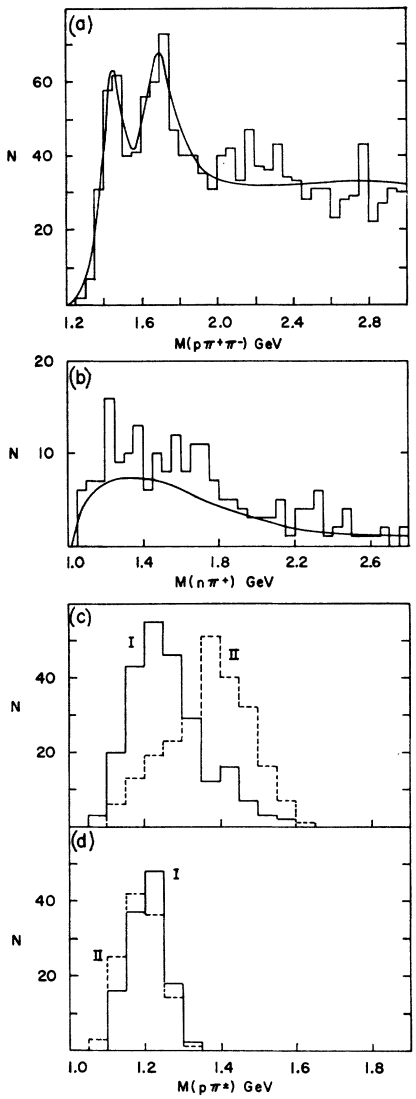

FIG. 1. (a) The $p\pi^+\pi^-$ mass distribution for reaction (2) for $M(p\pi^+\pi^-)\leq 3.0$ GeV. The smooth curve is the result of fitting the data with resonance expressions for the 1450- and 1700-MeV features plus a background formed with a Deck term and an additional polynomial form (see Refs. 1 and 3). (b) The $n\pi^+$ mass distribution for reaction (1). The smooth curve is a hand-drawn estimate of "background." (c) I, the $p\pi^+$ mass distribution for reaction (2) for events with $p\pi^+\pi^-$ mass in the 1600–1800-MeV region; II, the corresponding $p\pi^-$ mass distribution; (d) I, the $p\pi^+$ mass distribution for reaction (2) for events with $p\pi^+\pi^-$ mass in the 1450 ± 50-MeV band; II, the corresponding $p\pi^-$ mass distribution.

[7] This is interpreted to imply an essentially unambiguous association of final- and initial-state baryons, i.e., the forward-going final-state proton is associated with the projectile and the background-going proton with the target (in the c.m. system).

[8] The 1450-MeV feature is produced with a much sharper c.m. angular distribution than the 1700-MeV effect (or, equivalently, at lower t). See Ref. 1.

[9] S. M. Berman and M. Jacob, Phys. Rev. **139**, B1023 (1965).

[10] A. Donnachie, in *Proceedings of the Fourteenth International Conference on High-Energy Physics, Vienna, 1968*, edited by J. Prentki and J. Steinberger (CERN, Geneva, 1968), p. 139.

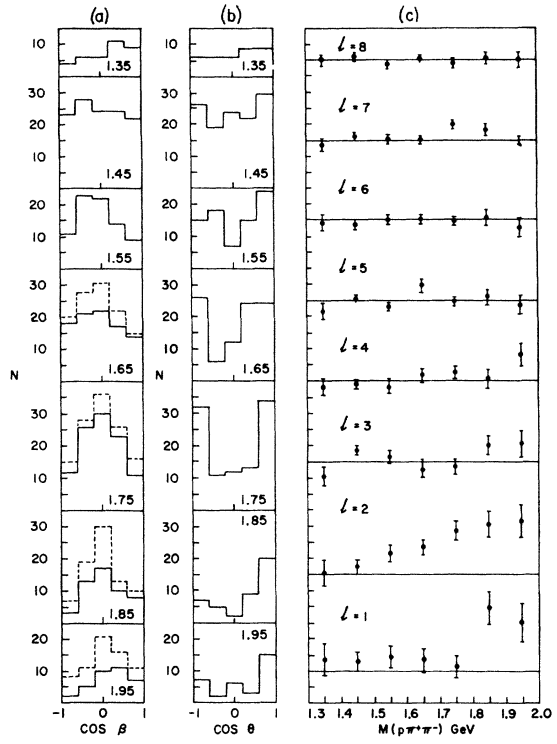

FIG. 2. Angular distributions and moments for reaction (2). See text for definitions of coordinate systems. (a) The polar angular distribution in the normal to the N^* decay plane for 0.1-GeV bands in $p\pi^+\pi^-$ mass from 1.3–2.0 GeV. The numbers on the graphs indicate the central masses of the bands. The solid and dashed histograms are obtained, respectively, with and without the additional requirement that the $p\pi^+$ mass be in the Δ^{++} region (1.225±0.125 GeV); (b) the polar angular distribution for $N^* \to \Delta^{++}\pi^-$ decay, again in 0.1-GeV bands for $p\pi^+\pi^-$ mass from 1.3–2.0 GeV. The $p\pi^+$ mass is in the Δ^{++} band (1.225±0.125 GeV). (c) The first eight normalized Legendre polynomial moments of the $N^* \to \Delta^{++}\pi^-$ polar angular distribution as a function of $p\pi^+\pi^-$ mass from 1.3–2.0 GeV.

the following analyses we compare the experimental decay angular distributions with theoretical predictions for these spin values under the assumption that the effects in question are dominated by decays of single resonance states. In particular, we do not consider effects of interference between states of different spin and parity.

II. SPIN ANALYSIS

A. Distribution in the Normal to the N^* Decay Plane

In Fig. 2(a) we present the polar angular distribution of the normal to the N^* decay plane as a function of $p\pi^+\pi^-$ mass from 1300 to 2000 MeV. (See part 1 of the Appendix for definition of the angles.) This is shown with and without the requirement that the $p\pi^+$ mass be in the Δ^{++} band. The character of the distributions is little affected by the Δ^{++} cut. Below 1500 MeV the distribution is relatively flat, while above 1500 MeV it develops an enhancement at $\cos\beta=0$, with an essentially symmetric depopulation at $\cos\beta=\pm1$.

TABLE I. Resume of fits[a] to distribution in the normal to the N^* decay plane for 1450- and 1700-MeV effects.

Enhancement	Spin	χ^2	χ^2 prob. (%)	ρ_{11}	Number of free parameters
1450 (I)[b]	$\frac{1}{2}$	11.1	2.5	$\frac{1}{2}$	0
1450 (II)[b]	$\frac{1}{2}$	11.6	24	$\frac{1}{2}$	0
1700	$\frac{3}{2}$	2.8	43	fixed at 0.5	1
	$\frac{5}{2}$	0.7	70	fixed at 0.5	2

[a] See part 1 of the Appendix for the theoretical expressions which are fitted to the distributions.
[b] The label 1450 (I) refers here to the folded distribution ($\cos\beta=0$ to $+1$) in five equal bins of width 0.2 in $\cos\beta$, while 1450 (II) refers to the unfolded distribution ($\cos\beta=-1$ to $+1$) in ten equal bins of width 0.2 in $\cos\beta$. (Also see Sec. II A.)

In the Appendix (part 1) the theoretical decay distributions for spins $\frac{1}{2}$, $\frac{3}{2}$, and $\frac{5}{2}$ are presented. The distribution for $p\pi\pi$ decay of a $J=\frac{1}{2}$ state is isotropic. The folded experimental decay distribution for the 1450±50-MeV $p\pi^+\pi^-$ mass region is shown in Fig. 3(a). The χ^2 probability for an isotropic fit to the distribution of Fig. 3(a) is 2.5%. It appears that the rather poor fit here is an accidental result of the choice of bins, since almost any other binning yields a much larger χ^2 probability. In particular, in using 10 bins from $\cos\beta=-1$ to $\cos\beta=+1$ we obtain a χ^2 of 11.6 corresponding to a χ^2 probability of 24% for 9 degrees of freedom. Our data for the 1450-MeV effect are thus consistent with a spin assignment of $J=\frac{1}{2}$. In previous work[1] this effect was identified with the $P_{11}(1470)$ resonance.

Contributions from decays of $J=\frac{1}{2}$ states with mass above 1500 MeV cannot be ruled out, but the striking anisotropy of the decay distributions clearly requires important contributions from states with $J\geq\frac{3}{2}$. In Fig. 3(b) is shown the folded distribution in the normal

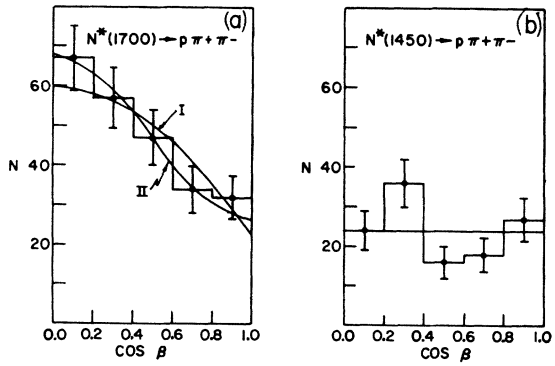

FIG. 3. (a) The folded polar angular distribution in the normal to the N^* decay plane for the 1700-MeV effect (1600–1800-MeV band). The curves shown are fits to the data using theoretical expressions for: I, N^* spin $\frac{3}{2}$ with $\rho_{11}=\frac{1}{2}$; II, N^* spin $\frac{5}{2}$ with $\rho_{11}=\frac{1}{2}$. (b) The folded polar angular distribution in the normal to the N^* decay plane for the 1450-MeV effect (1450±50-MeV cut). The curve shown is a fit to the data using the theoretical expression for N^* spin $\frac{1}{2}$.

to the N^* decay plane for events with $p\pi^+\pi^-$ mass in the 1600–1800-MeV region. The smooth curves on Fig. 3(b) are fits to the data using the theoretical expressions for N^* spin $\frac{3}{2}$ and $\frac{5}{2}$ with the restriction that $\rho_{11}=\frac{1}{2}$. The application of this condition serves to reduce the number of free parameters to one for the $J=\frac{3}{2}$ case and two for the $J=\frac{5}{2}$ case and is, moreover, consistent with the results of Sec. II C, in which the best fits to the sequential distribution are obtained with $\rho_{11}=\frac{1}{2}$. Our results for the fits here are: for $J=\frac{3}{2}$, $\chi^2=2.8$ and a χ^2 probability of 43% for 3 degrees of freedom; for $J=\frac{5}{2}$, $\chi^2=0.7$ and a χ^2 probability of 70% for 2 degrees of freedom. On the basis of this analysis we favor $J=\frac{5}{2}$, but both $J=\frac{5}{2}$ and $J=\frac{3}{2}$ provide quite acceptable fits. Results of these fits for both the 1700- and 1450-MeV effects are summarized in Table I.

B. Legendre Polynomial Moments

The first eight normalized Legendre polynomial moments of the polar angular distribution for $N^*\to\Delta^{++}\pi^-$ are presented in Fig. 2(c), as a function of $p\pi^+\pi^-$ mass. (See part 2 of the Appendix for definition of the polar angle.) Of the even moments, only that for $L=2$ deviates significantly from zero. This moment is near zero below 1500 MeV, but grows larger above 1500 MeV. We conclude from this that an L value of at least one is involved in the $\Delta\pi$ system in the 1700-MeV mass band, which, in conjunction with the expected isotropic distribution for $J=\frac{1}{2}$ (see Sec. II C), implies that $J\geq\frac{3}{2}$ for important contributing states. Further implications of this result are discussed in Sec. II D.

C. Sequential Decay Distributions: $N^*\to\Delta\pi$, $\Delta\to p\pi$

The polar angular distribution for $N^*\to\Delta^{++}\pi^-$ is presented in Fig. 2(b), again as a function of $p\pi^+\pi^-$ mass. (See part 2 of the Appendix for definition of the angles.) Below 1500 MeV the distributions are essentially isotropic, while above 1500 MeV they exhibit a fairly symmetrical and, in some cases, pronounced peaking at $\cos\theta=\pm1$. The polar angular distribution (see Appendix) for the $\Delta^{++}\pi^-$ decay of a spin-$\frac{1}{2}$ state is also isotropic, so the immediate conclusion here is quite the same as that from the distribution in the normal to the N^* decay plane (Sec. II A), i.e., the data are consistent with $J=\frac{1}{2}$ for the 1450-MeV effect but require $J\geq\frac{3}{2}$ for $p\pi\pi$ mass above 1500 MeV.

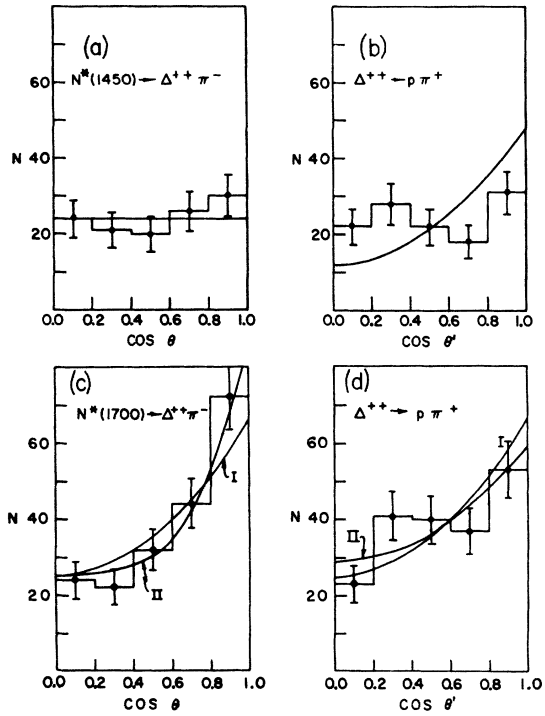

FIG. 4. (a) The folded polar angular distribution for $N^*\to\Delta^{++}\pi^-$ for events with $p\pi^+\pi^-$ mass in the 1450±50-MeV band and $p\pi^+$ mass in the Δ^{++} band (1225±125 MeV). (b) The polar angular distribution for $\Delta^{++}\to p\pi^+$ for similarly selected events. The curves on (a) and (b) are results of fitting both distributions simultaneously with theoretical expressions for N^* spin $\frac{1}{2}$. (c) The folded polar angular distribution for $N^*\to\Delta^{++}\pi^-$ for events with $p\pi^+\pi^-$ mass in the 1600–1800-MeV band and $p\pi^+$ mass in the Δ^{++} band (1225±125 MeV). (d) The polar angular distribution for $\Delta^{++}\to p\pi^+$ for similarly selected events. Curves I on (c) and (d) are results of fitting both distributions simultaneously with theoretical expressions for N^* spin $\frac{3}{2}$, while the curves II are for analogous fits for N^* spin $\frac{5}{2}$, with $\rho_{55}=0$.

The folded experimental decay distribution for $N^*\to\Delta\pi$ for the 1450±50-MeV region is shown in Fig. 4(a). The χ^2 probability for an isotropic fit to this distribution is 55%. The assumption of $J=\frac{1}{2}$ for the 1450-MeV effect implies, for the $\Delta^{++}\pi^-$ decay, that the diagonal density matrix elements of the daughter Δ^{++} have the values $\rho_{11}'=\frac{1}{2}$, and $\rho_{33}'=0$. The decay distribution for $\Delta^{++}\to p\pi^+$ is thus required to have the form $1+3\cos^2\theta'$. The experimental decay distribution for $\Delta^{++}\to p\pi^+$ is shown in Fig. 4(b) with the curve $1+3\cos^2\theta'$ normalized to the data. The χ^2 for this fit is 24.3, corresponding to a χ^2 probability of 0.005%. Using a different choice of bins (10 equal bins from $\cos\theta'=-1$ to $+1$), we obtain a χ^2 of 30.8, corresponding to a χ^2

TABLE II. Resume of joint fits[a] to $N^*\to\Delta^{++}\pi^-$ and $\Delta^{++}\to p\pi^+$ polar angular distributions for the 1450-MeV effect.

Analysis procedure	Spin	χ^2	χ^2 prob. (%)
Gross (I)[b]	$\frac{1}{2}$	28	0.05
Gross (II)[c]	$\frac{1}{2}$	33.5	0.1
Reconstructed[d]	$\frac{1}{2}$	19.8	1.1

[a] See part 2 of the Appendix for the theoretical expressions which are fitted to the data. The χ^2's quoted here are the sums of those for fits to the $N^*\to\Delta^{++}\pi^-$ distribution and $\Delta^{++}\to p\pi^+$ distribution. There are no variable parameters.

[b] Gross (I) refers to a fit to the distributions for all events having $p\pi^+\pi^-$ mass in the 1450±50-MeV band and $p\pi^+$ mass in the 1225±125-MeV band. The $p\pi^+$ distribution is folded ($\cos\theta'=0$ to $+1$) in five equal bins of width 0.2 in $\cos\theta$.

[c] Gross (II) is analogous to gross (I) save that the $p\pi^+$ distribution is unfolded ($\cos\theta'=-1$ to $+1$) in ten equal bins of width 0.2 in $\cos\theta'$.

[d] The fit here is to background-free distributions for the 1450-MeV effect constructed from distributions from the 1450±50-MeV band and 1350±50- and 1550±50-MeV cuts, using estimates of background and 1450-MeV effect contributions in each region determined from fits (Refs. 1 and 3).

TABLE III. Resume of joint fits[a] to $N^* \to \Delta^{++}\pi^-$ and $\Delta^{++} \to p\pi^+$ polar angular distributions for the 1700-MeV effect.

Analysis procedure	Spin	χ^2	χ^2 prob. (%)	ρ_{11}[a]	ρ_{11}'	R[b]
Gross[c]	$\frac{3}{2}$	13.1	4.2	$0.5_{-0.02}$[a]	$0.40_{-0.01}{}^{+0.07}$	$6.3_{-2.6}{}^{+7.1}$
	$\frac{5}{2}$	6.6	36	$0.5_{-0.12}$[a]	$0.37_{-0.05}{}^{+0.05}$	$2.7_{-1.0}{}^{+2.2}$
Reconstructed[d]	$\frac{3}{2}$	8.3	22	$0.5_{-0.04}$[a]	$0.43_{-0.05}{}^{+0.07}$	$6.0_{-2.7}{}^{+13.0}$
	$\frac{5}{2}$	3.8	70	$0.5_{-0.16}$[a]	$0.35_{-0.06}{}^{+0.06}$	$2.3_{-0.9}{}^{+1.9}$

[a] See part 2 of the Appendix for the theoretical expressions which are fitted to the data. The χ^2's quoted here are sums of those for the fits to $N^* \to \Delta^{++}\pi^-$ and $\Delta^{++} \to p\pi^+$ distributions. Two parameters, ρ_{11} and ρ_{11}', are adjusted in the fitting procedure. They are permitted to vary only over the physically allowed range. Errors in parameters are set by the points at which (for variation of a single parameter) the χ^2 probability is one-half of that at minimum. For ρ_{11} the minimum occurs in all cases for a value equal to or exceeding the physically permitted maximum 0.5 so only the lower error limit is given.

[b] $R \equiv \rho_{11}'/(\frac{1}{2} - \rho_{11}') \equiv |F_{1/2}|^2/|F_{3/2}|^2$ (see part 2 of the Appendix).

[c] The fit is made to distributions for all events having $p\pi^+\pi^-$ mass in the 1600–1800-MeV band and $p\pi^+$ mass in a 1225±125-MeV band.

[d] The fit is to a background-free distribution for the 1700-MeV effect constructed from distributions for the 1600–1800-MeV band and the 1500–1600- and 1800–1900-MeV cuts, using estimates of background and 1700-MeV effect contributions in each region determined from fits (Refs. 1 and 3).

probability of 0.03%. The results of a *joint* fit to both the $N^* \to \Delta^{++}\pi^-$ and $\Delta^{++} \to p\pi^-$ decay angular distributions are summarized in Table II. The quality of the joint fit is in this case effectively determined by that of the fit to the $\Delta^{++} \to p\pi^+$ distribution. Possible effects of background have been in part taken into consideration in the following manner: We use estimates of the contribution (based on fits to the $\Delta^{++}\pi^-$ distributions[3]) of the 1450-MeV effect in both the 1450±50-MeV region and in neighboring cuts to construct an approximately "background-free" decay angular distribution for the 1450-MeV feature. Results of the joint fit to this reconstructed distribution are included in Table II. The suitability of this background correction procedure may be questioned from the point of view of the correctness of the representation of the $\Delta^{++}\pi^-$ mass distribution as a Deck background plus 1450- and 1700-MeV effects, as discussed in Ref. 3. In any case, the conclusions with regard to the $\Delta^{++} \to p\pi^+$ decay distribution for the 1450-MeV effect do not depend critically on this point. The $1+3\cos^2\theta'$ fit is poor both with and without background correction. Two possible interpretations of this are (1) that the 1450-MeV effect is not dominantly $J=\frac{1}{2}$, or (2) that $\Delta\pi$ is not the principal decay mode of the 1450-MeV effect. The latter possibility is not in conflict with remarks made in Sec. II A. Further implications of this result are discussed in Sec. II E.

We now consider in detail the sequential decay of the 1700-MeV effect. The theoretical form for the $N^* \to \Delta^{++}\pi^-$ polar angular distributions for N^* spins $\frac{3}{2}$ and $\frac{5}{2}$ involves, in addition to the N^* density matrix elements, another parameter (referred to as R) which is the ratio ρ_{11}'/ρ_{33}' of density matrix elements of the daughter Δ^{++} referred to the Δ^{++} direction (see Appendix). Figure 4(d) is the folded experimental polar angular distribution for $\Delta^{++} \to p\pi^+$ for events with $p\pi^+\pi^-$ mass in the 1600–1800-MeV region, while in Fig. 4(c) is displayed the $N^* \to \Delta^{++}\pi^-$ polar angular distribution for the same $p\pi^+\pi^-$ mass cut. We have obtained simultaneous fits to both distributions for spin hypotheses of $\frac{3}{2}$ and $\frac{5}{2}$ for the parent N^*. These are two-parameter fits in both cases, involving ρ_{11} of the parent N^* and ρ_{11}' of the daughter Δ^{++}. For $J=\frac{5}{2}$, ρ_{55} is taken to be zero.[11] The curves resulting from the fits are shown on the figures, and the fitted values of the density matrix elements for both N^* and Δ^{++}, as well as the χ^2 and χ^2 probability, are presented in Table III. On the basis of this analysis, $J=\frac{5}{2}$ is preferred over $J=\frac{3}{2}$. These results are based on all $\Delta^{++}\pi^-$ events in the 1600–1800-MeV $p\pi^+\pi^-$ mass band, with no correction for background. We have considered also in this case the possible effects of background. Using estimates (based on fits to the $\Delta^{++}\pi^-$ distributions[3]) of the contribution of the 1700-MeV effect and of background in both the 1600–1800-MeV $p\pi^+\pi^-$ mass region and in adjoining bands, we can construct an approximately background-free decay angular distribution for the 1700-MeV feature. The results of fitting these distributions in the manner previously described are included also in Table III. The conclusions here are essentially the same as those from the fit to the uncorrected data. In this connection, we note that the decay angular distributions for the background are not strikingly different from those for the 1700-MeV effect itself. This suggests that treatment of the data in terms of resonances plus Deck background may not be entirely appropriate here.[3]

D. Parity of 1700-MeV Effect

The results of our moment analysis (Sec. II B) are consistent with the assumption that the highest significant partial wave in the $\Delta^{++}\pi^-$ system (for the 1700-MeV feature) is $L=1$, though this is not required to be the case. Clearly, $L=0$ is not dominant, for if it were the spin of the N^* system would be $\frac{3}{2}^-$ and the decay angular distribution for $N^* \to \Delta^{++}\pi^-$ would be essentially flat, as discussed in Sec. II E.

We consider here implications of the assumption that $L=1$ is the only strongly contributing partial wave. An important result of this hypothesis is a condition on R, the ratio of the squared magnitudes of the helicity amplitudes. We may use results of Jacob and Wick[12] to relate the amplitudes appearing in the helicity formulation for the $N^* \to \Delta^{++}\pi^-$ decay with those appearing in the LS coupling expansion. For dominant $L=1$ in the $\Delta^{++}\pi^-$ decay the N^* spin and parity are either $\frac{3}{2}^+$ or $\frac{5}{2}^+$. For these two cases the relations between the helicity and LS amplitudes are given in part 3 of the Appendix. For $L=1$ dominant, $R=0.111$ for $\frac{3}{2}^+$ and 1.5 for $\frac{5}{2}^+$. These are to be compared with experimental R values of $6.0_{-2.7}{}^{+13}$ for $\frac{3}{2}^+$ and $2.3_{-0.9}{}^{+1.9}$ for $\frac{5}{2}^+$ determined from fits to the $N^* \to \Delta^{++}\pi^-$ and $\Delta^{++} \to p\pi^+$ decay distri-

[11] In the reaction $pp \to N^*p$, where N^* is produced strongly forward (or backward), the maximum spin projection of the N^* is $\pm\frac{3}{2}$ along the beam direction.

[12] M. Jacob and G. C. Wick, Ann. Phys. (N. Y.) 7, 404 (1959).

butions (reconstructed) discussed in Sec. II C and summarized in Table III. On the basis of th is analysis $J^P=\frac{5}{2}^+$ is preferred for the 1700-MeV feature.

E. Implications of Spin Analysis for Δ^{++} Decay of 1450-MeV Effect

For the 1450-MeV region the moment analysis of Sec. II B is easily consistent with an S-wave decay into $\Delta^{++}\pi^-$. This is reflected again in the flat polar angular distribution for $N^*(1450)\to\Delta^{++}\pi^-$ observed in Sec. II C. If, however, the 1450-MeV effect decays into the $\frac{3}{2}^+$ Δ^{++} and a 0^- pion with relative orbital angular momentum 0, then its spin is $\frac{3}{2}^-$. In a $\frac{3}{2}^-$ decay into $\frac{3}{2}^+ + 0^-$ an assumed $L=0$ dominance implies $R=1$ (see Appendix), which leads to an isotropic $N^*\to\Delta^{++}\pi^-$ polar angular distribution, independent of ρ_{11}, and also to an isotropic $\Delta^{++}\to p\pi^+$ polar angular distribution, which is, in fact, in good agreement with the data discussed in Sec. II C and presented in Figs. 4(a) and 4(b). As we pointed out in Sec. II C, the flat experimental $\Delta^{++}\to p\pi^+$ decay is inconsistent with the alignment expected for a Δ^{++} arising in decay of a $\frac{1}{2}^+$ N^* system. We can summarize our results in the following statements: (1) If the 1450-MeV effect in our data has spin $\frac{1}{2}$, then we favor only a weak $\Delta^{++}\pi^-$ decay branching; (2) if this effect does have a strong $\Delta^{++}\pi^-$ decay, we favor $J^P=\frac{3}{2}^-$. With regard to this latter possibility, we note that the nearest $\frac{3}{2}^-$ state is the $D_{13}(1515)$. If the 1450-MeV effect in our data has spin $\frac{1}{2}^+$ and does not have a dominant $\Delta^{++}\pi^-$ branching, one must consider the possibility of a strong σp branching, where σ refers to the $I=0$, $J^P=0^+$ dipion resonance.[13] We have examined the $\pi^+\pi^-$ mass distribution (not shown) for events with at least one $p\pi^+\pi^-$ mass combination in the 1450±50-MeV band. This distribution exhibits no significant deviations from phase space; in particular, it does not show the broad peaking at around 500 MeV characteristic of the $\pi^+\pi^-$ mass distribution from the reaction $\pi^-p\to\pi^-\pi^+n$[13] at a c.m. energy near 1450 MeV.

III. ELASTICITY ARGUMENTS FOR 1450- AND 1700-MeV EFFECTS

In associating the $p\pi\pi$ effects in our data with resonances inferred from phase-shift analysis,[10] there is an additional point bearing on the question of the spin, one connected with the elasticities of candidate states. Considering the process $pp\to N^*p$, one expects that certain of the inelastic N^* decay modes lead to a $pp\pi^+\pi^-$ final state, while one of the elastic decays contributes to the $pn\pi^+$ state. Our $n\pi^+$ mass distribution for reaction (1) is presented in Fig. 1(d).

The statistical reliability of the data is poor, but it is clear from Fig. 1(b) that there are no striking enhancements in either the 1450±50- or 1600–1800-MeV regions. Using simple bin-averaging techniques to smooth the data, we do find evidence for a local enhancement in the 1600–1800-MeV band which is superposed on the general trend of the data to rise to a broad maximum at around 1200–1300-MeV (the Δ^+ region). This procedure gives no evidence for a sharp 1400-MeV peak. The total number of events in the 1450±50-MeV region of the $n\pi^+$ mass distribution is 16, while that in the 1600–1800-MeV band is 37. If possible resonance contributions in these regions are considered to be superposed on some kind of background, then these numbers must be considered as upper limits. For our purposes here we have put on Fig. 1 an estimated smooth background which is normalized to locally low portions of the histogram at 1200, 1425, and 2000 MeV. Above this background the contributions of the 1450- and 1700-MeV features are approximately 4 and 15 events, respectively.

If we associate a signal in the $p\pi^+\pi^-$ mass distribution with a particular resonance of known isotopic spin and elasticity, we can estimate its contribution in our $n\pi^+$ distribution. In the case of the 1450-MeV effect, this procedure is complicated by the manner in which the data sample is selected for reaction (1). Our sample of $pn\pi^+$ events is chosen to have an identified (slow) lab proton and neutrons with lab momentum in excess of 4 GeV/c, which effectively permits observation of only the forward-going $N^*(1450)$. The t dependence of the $N^*(1450)$ production is sufficiently strong (see Ref. 1), however, so that most events of this type involve short stopping protons for which our measuring efficiency is considerably reduced. We have estimated the efficiency for obtaining forward-going $N^*(1450)$ events by comparison of separate $p\pi^+\pi^-$ spectra from reaction (2) for forward- and backward-going $p\pi^+\pi^-$ systems. This provides an upper limit for $N^*(1450)$ production in reaction (1), since an unmeasured or poorly measured track places an event, at best, in the zero-constraint class with respect to a $pn\pi^+$ fit.

As indicated previously, we have identified the 1450-MeV $p\pi^+\pi^-$ effect in our data with the $P_{11}(1470)$ state, whose elasticity is 0.57.[10] The isospin coupling in the $p\pi^+\pi^-$ decay of this state must be considered unknown in view of the question raised in Sec. II C about the $\Delta^{++}\pi^-$ decay branching. The $I=\frac{1}{2}$ $N\pi\pi$ state may be formed through an intermediate $I=\frac{1}{2}$ or $I=\frac{3}{2}$ πN coupling or through a complex admixture of both with a variable phase factor. The difference between *pure* $I=\frac{1}{2}$ or *pure* $I=\frac{3}{2}$ coupling in respect to the strength of the $p\pi^+\pi^-$ decay is only 20%. Disregarding possible interference effects, we simply take the average of the results for the pure $I=\frac{1}{2}$ and pure $I=\frac{3}{2}$ cases. On the basis of these considerations the expected contribution of this state in the 1450±50-MeV band of our $n\pi^+$ distribution is less than 16 events. This result is not in serious disagreement with the estimated ~4 events in this region of the $n\pi^+$ mass distribution, considering the

[13] N. Barish-Schmidt, A. Barbaro-Galtieri, LeRoy R. Price, A. H. Rosenfeld, P. Söding, C. G. Wohl, Matts Roos, and Gianni Conforto, Rev. Mod. Phys. 41, 109 (1969).

various uncertainties involved; however, the lack of a sharp 1450-MeV signal is puzzling.

For the 1700-MeV effect the preferred spin and parity, on the basis of the analysis of Secs. II A–II C, is $\frac{5}{2}^+$. This feature is most consistently associated with the $F_{15}(1690)$ resonance. Using the elasticity of 0.61 for this state inferred from phase-shift analysis[10] and assuming pure $I=\frac{3}{2}$ intermediate πN coupling, we estimate 41 events in the 1600–1800-MeV band of our $n\pi^+$ distribution. Problems associated with determination of the efficiency for observing forward-going N^* systems are less critical for the 1700-MeV feature than for the 1450-MeV effect, due to the generally higher t of the former (see Refs. 1 and 8). Nevertheless, considering uncertainties in the phase-shift estimates of the elasticity (ranging from 0.54 to 0.68) for the $F_{15}(1690)$ and uncertainty in background estimates in our data, we cannot claim that there is a serious discrepancy here.

IV. CONCLUSIONS AND DISCUSSION

Our data for the 1450-MeV effect are consistent with the assumption of spin $\frac{1}{2}$ providing that the $\Delta^{++}\pi^-$ branching is assumed to be small. On the other hand, a large $\Delta^{++}\pi^-$ decay mode implies $J^p=\frac{3}{2}^-$ for this feature. Our mass for the 1450-MeV peak, 1443±15 MeV, is in good agreement with that of the $P_{11}(1470)$ πN resonance inferred from phase-shift analyses, but the width, 100±15 MeV, is considerably less than the 260 MeV given by the phase-shift work. The ratio of the contributions of this effect in the $pp\pi^+\pi^-$ and $pn\pi^+$ reactions is marginally consistent with the elasticity of the $P_{11}(1470)$.

For the 1700-MeV effect the preferred spin and parity, $J^p=\frac{5}{2}^+$, and the experimental mass, 1693±15 MeV, favor an identification with the $F_{15}(1690)$ state. However, our width, 235±50 MeV, is considerably in excess of that given for the $F_{15}(1690)$ resonance from phase-shift work, 125 MeV. The relative contribution of this effect in our reactions (1) and (2) is, again, marginally consistent with the elasticity of the $F_{15}(1690)$ state.

We have no explanation for the difference between our experimental widths and the accepted widths for these two effects, assuming that the identification with established πN resonances is correct. It is clearly not connected with resolution, since one of the two effects is considerably more narrow, and the other considerably wider than expected. We note here that the widths of effects (which have been associated with these same states) seen by other workers using both bubble-chamber and counter techniques have varied considerably.

The general effects of interference arising in the production and decay of the many states of different spin and parity which lie in the region of interest are not treated here. The additional parameters and/or special assumptions which must be introduced in such a discussion render the results largely inconclusive. We cannot exclude the possibility that the data presented here might be better characterized in terms of a significant interference between two or more contributing resonance systems rather than arising, as we have discussed it, from a dominant contribution from single states.

It is worth noting here that the fact that both effects are produced at low t and can be reasonably associated with $I=\frac{1}{2}$ positive-parity states is consistent with the view that they are produced by diffraction dissociation[14] of one (or the other) of the incident protons. Diffraction dissociation in high-energy processes is often considered to arise through exchange of a 0^+ system. One implication of this assumption for the reactions of interest here is that the maximum spin projection along the beam (for forward production) of the final-state N^* system is $\pm\frac{1}{2}$. Our results in this analysis are in good agreement with this approach, since the N^* decay angular distributions discussed in Sec. II C are best fit for $\rho_{11}=\frac{1}{2}$.

ACKNOWLEDGMENTS

The authors gratefully acknowledge the assistance of members of the Brookhaven National Laboratory staff in obtaining the film on which this work is based and the efforts of the scanning, programming, and technical support groups at Iowa State University.

APPENDIX

We present here various theoretical resonance-decay angular distributions. Certain of these expressions are special cases of general formulas derived by Berman and Jacob[9] (referred to here as BJ). In the following, the symbol $\rho_{2n,2m}$ refers to the n, m element of the N^* density matrix in the N^* rest frame. The z axis to which this N^* density matrix is referred is the direction of the initial-state proton which is associated with the N^*, in the N^* rest frame (see Ref. 7).

1. Distribution in the Normal to the $p\pi\pi$ Decay Plane for $N^*\to p\pi\pi$

The polar angle β is defined as the angle between the normal to the $p\pi^+\pi^-$ decay plane (for the decay $N^*\to p\pi^+\pi^-$) and the direction of the associated-initial-state proton, all in the N^* rest frame. The theoretical decay distributions in the angle β for decays of N^*'s with $J=\frac{1}{2}$, $\frac{3}{2}$, and $\frac{5}{2}$ are

$J=\frac{1}{2}$:

$$N(\beta)=\text{const}, \tag{A1}$$

$J=\frac{3}{2}$:

$$N(\beta)=\tfrac{1}{4}[\rho_{11}+G(\tfrac{1}{2}-\rho_{11})](1+3z^2)+\tfrac{3}{4}[G\rho_{11}+(\tfrac{1}{2}-\rho_{11})](1-z^2), \tag{A2}$$

[14] T. T. Chou and C. N. Yang, Phys. Rev. **175**, 1832 (1968).

$J=\frac{5}{2}$ (restricting $\rho_{33}=\rho_{55}=0$):

$$N(\beta)=(10z^4-4z^2+2)+G(-15z^4+14z^2+1)+G'(5z^4-10z^2+5), \quad \text{(A3)}$$

where $z=\cos\beta$, and where $G\equiv R_{3/2}{}^+/R_{1/2}{}^+$ and $G'\equiv R_{5/2}{}^+/R_{1/2}{}^+$. The R's are phenomenological decay parameters defined in BJ; here ρ_{11} and the G's are treated as parameters determined by fitting the data. The allowed ranges are $0\leq\rho_{11}\leq\frac{1}{2}$, $0\leq G\leq\infty$. Expressions (A1) and (A2) are special cases of BJ Eq. (14) obtained by (1) integrating over the azimuthal angle α, (2) using $\rho_{nm}=(-1)^{n-m}\rho_{-n-m}$, and (3) using $\sum\rho_{nn}=1$. The parity of the decaying N^* does not appear in the expressions for the $p\pi^+\pi^-$ polar angular distributions.

2. Sequential Decay Distribution

For the sequential decay $N^*\to\Delta^{++}\pi^-$, $\Delta^{++}\to p\pi^+$, we define two polar decay angles. The angle θ refers to the $N^*\to\Delta\pi$ decay and is defined as the angle between the direction of the Δ^{++} and the direction of the initial-state proton associated with the N^*, all in the N^* rest frame. The angle θ' refers to the daughter decay $\Delta^{++}\to p\pi^+$ and is defined as the angle between the Δ^{++} direction and the final-state π^+ direction, in the Δ^{++} rest frame. The density matrix elements of the Δ^{++} are called $\rho_{2n,2m}{}'(\theta)$ and are referred to a z axis which is the direction of the Δ^{++}. The $\rho_{2n,2m}{}'(\theta)$ describe the decay of the Δ in its own rest frame. Figure 5 of BJ illustrates such a sequential decay.

Denoting the theoretical polar angular distribution for the decay $N^*\to\Delta^{++}\pi^-$ by $I(\theta)$, and the distribution for the secondary decay $\Delta^{++}\to p\pi^+$ by $I'(\theta')$, we have, for N^* spins $\frac{1}{2}$, $\frac{3}{2}$, and $\frac{5}{2}$,

$J=\frac{1}{2}$:

$$I(\theta)=\text{const}, \quad \text{(A4)}$$

$$I'(\theta')=1+3y^2, \quad \text{(A5)}$$

$J=\frac{3}{2}$:

$$I(\theta)=(\tfrac{1}{2}-\rho_{11})[(1+3x^2)+3R(1-x^2)]+\rho_{11}[3(1-x^2)+R(1+3x^2)], \quad \text{(A6)}$$

$$I'(\theta')=(\tfrac{3}{4}-\langle\rho_{11}{}'\rangle)+3(\langle\rho_{11}{}'\rangle-\tfrac{1}{4})y^2, \quad \text{(A7)}$$

$J=\frac{5}{2}$ (restricting $\rho_{55}\equiv 0$):

$$I(\theta)=(\tfrac{1}{2}-\rho_{11})[R(1+14x^2-15x^4)]+\tfrac{1}{2}(9-38x^2+45x^4)+\rho_{11}[R(2-4x^2+10x^4)+(1+14x^2-15x^4)], \quad \text{(A8)}$$

$I'(\theta')=$ same as (A7),

where $x\equiv\cos\theta$, $y\equiv\cos\theta'$, $\langle\rho_{11}{}'\rangle\equiv\int\rho_{11}{}'(\theta)dx$, and where

$$R\equiv\langle\rho_{11}{}'\rangle/(\tfrac{1}{2}-\langle\rho_{11}{}'\rangle)\equiv|F_{1/2}|^2/|F_{3/2}|^2. \quad \text{(A9)}$$

Here $F_{1/2}$ and $F_{3/2}$ are helicity amplitudes appearing in the theoretical expressions of BJ. The allowed ranges of the parameters ρ_{11} and $\langle\rho_{11}{}'\rangle$ are 0–$\frac{1}{2}$. Formulas (A4), (A6), and (A8) are obtained from BJ Eq. (48), while (A7) is the well-known Δ^{++} polar decay distribution. In deriving (A4)–(A8), use was made of (1) $I(\theta)=\int d\varphi\sum\rho_{nn}{}'(\theta,\varphi)$, (2) $\rho_{nm}=(-1)^{n-m}\rho_{-n-m}$, (3) $\sum\rho_{nn}=1$, (4) $\langle\rho_{nm}{}'\rangle=(-1)^{n-m}\langle\rho_{-n-m}{}'\rangle$, and (5) $\sum\langle\rho_{nn}{}'\rangle=1$. The parity of the decaying N^* does not appear in the theoretical expressions for the decay distributions. Note that in the text $\langle\rho_{mm}{}'\rangle$ is replaced by $\rho_{mm}{}'$.

3. Relation between Helicity and LS Coupling Amplitudes for $N^*\to\Delta^{++}\pi^-$

Using results from Jacob and Wick,[12] we obtain the following formal connection between the helicity amplitudes F_λ and the LS amplitudes B_L for the decay of an N^* system of spin J into a spin-$\frac{3}{2}$ particle and a spin-0 particle:

$$F_\lambda=\sum_L B_L\left(\frac{2L+1}{2J+1}\right)^{1/2}\langle L,0;\tfrac{3}{2},\lambda|J,\lambda\rangle.$$

Application of this relation to cases of interest in the text gives:

$J=\frac{3}{2}^+$ ($L=1$ and 3):

$$F_{1/2}=\frac{1}{2\sqrt{5}}(B_1+3B_3), \quad F_{3/2}=\frac{1}{2\sqrt{5}}(3B_1-B_3).$$

For $B_3=0$ we obtain $R=|F_{1/2}|^2/|F_{3/2}|^2=1/9$.

$J=\frac{3}{2}^-$ ($L=0$ and 2):

$$F_{1/2}=\tfrac{1}{2}(B_0-B_2), \quad F_{3/2}=\tfrac{1}{2}(B_0+B_2).$$

For $B_2=0$ we obtain $R=|F_{1/2}|^2/|F_{3/2}|^2=1$.

$J=\frac{5}{2}^+$ ($L=1$ and 3):

$$F_{1/2}=\frac{1}{\sqrt{30}}(3B_1-B_3\sqrt{6}), \quad F_{3/2}=\frac{1}{\sqrt{30}}(B_1\sqrt{6}+3B_3).$$

For $B_3=0$ we obtain $R=|F_{1/2}|^2/|F_{3/2}|^2=\frac{3}{2}$.